#### **NURETH14-510**

# ANALYSIS of THERMAL STRATIFICATION in the UPPER PLENUM of the MONJU REACTOR VESSEL

#### T. Sofu and J. Thomas

Argonne National Laboratory, Illinois, U.S.A.

#### Abstract

An analysis of sodium circulation in the upper plenum of Monju fast reactor has been performed for validation of the multi-dimensional computational fluid dynamics (CFD) models using data from the turbine trip test conducted in December 1995. A simplified symmetric segment of the upper plenum model has been used with explicit geometric representation of the holes on the inner barrel to simulate the bypass flow. The calculations for the steady-state and transient conditions are performed and compared with the thermally stratified flow conditions observed during the test. Reasonable agreement with test data is observed for steady-state solutions. However, CFD simulations with various modeling options consistently predict a faster dissolution of the thermal stratification than the test data indicates, probably due to underestimating the bypass flow.

#### Introduction

Argonne National Laboratory (ANL) is participating in an international benchmark for analysis of thermal stratification in the upper plenum of the Monju reactor vessel. Organized by the International Atomic Energy Agency (IAEA) as a coordinated research project, this activity aims at validation of the multi-dimensional CFD models for assessment of passive safety in sodium-cooled fast reactors. The benchmark is sponsored by JAEA (Japan) and, in addition to Argonne, participated by CEA (France), KAERI (Republic of Korea), IPPE (Russia), IGCAR (India), and CIAE (China). Although not formally within the IAEA framework, the benchmark evaluations are also independently pursued by researchers at JAEA and University of Fukui (Japan).

Monju, located near Tsuruga, Japan, is a MOX-fueled, loop-type 714 MW-thermal (280 MW-electric) sodium-cooled fast reactor with three primary coolant circuits. The project involves the modeling of sodium flow and thermal stratification phenomena that were measured in the upper plenum during the turbine trip test conducted in December 1995. During the first phase of the project, a simplified 1/6 symmetric upper plenum model has been developed as the baseline for evaluation of the candidate CFD software using a consistent, common geometry. The holes on the inner vessel barrel are modelled explicitly as alternate flow paths to the down-comer region, bypassing the thermally stratified portion of the upper plenum. The complex geometric structures above the core are represented using the porous media approach.

At Argonne, the reference case simulations are performed with the STAR-CD software [1] using the high-Reynolds number realizable k- $\epsilon$  turbulence model in conjunction with logarithmic wall-functions to simulate the viscous sub-layer on the solid component surfaces. This paper provides a summary of the efforts performed to date and the results of the evaluations with the simplified model using various assumptions and options in support of Argonne participation in this IAEA coordinated research project.

### 1. Description of Monju Upper Plenum

The core of the Monju reactor consists of conventional driver fuel assemblies with two enrichment zones, blanket fuel assemblies, neutron shields and control rods. Liquid sodium coolant is fed to the core through three inlet nozzles located at the lower plenum and flows out of the vessel through three outlet nozzles located in the upper plenum. In addition to the reactor core, the other main components in reactor vessel include the core barrel, upper core structures, dip-plate, inner-barrel with two rows of bypass holes, the fuel handling and transfer machines, in-vessel spent fuel racks, and three inlet and outlet nozzles (one for each loop) as shown in Figure 1.

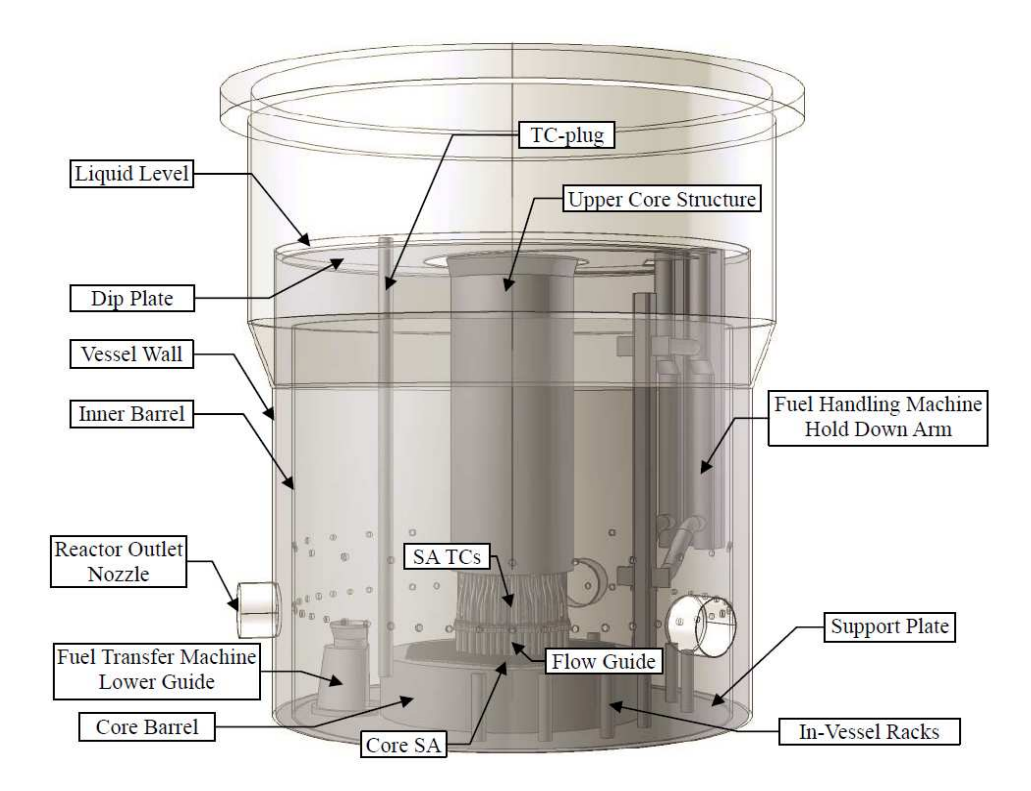


Figure 1 Diagram of Monju upper plenum.

Since thermal stratification was limited to the upper plenum, only the portion of the reactor vessel above the core support plate is considered in this analysis. The cylindrical support plate separates the upper and lower plena and supports the inner barrel. The stainless-steel reactor vessel is a vertical cylinder approximately 7 m in diameter. The sodium is nominally filled up to a level of 6,930 mm above the support plate, but a dip-plate is immersed just below the top surface to limit the impact of any sloshing or cover gas entrainment due to formation of a vortex. Three outlet nozzles, one for each primary system loop, penetrate the reactor vessel symmetrically.

The stainless-steel inner barrel separates the riser region of the plenum (above the core) from the downcomer region (annulus connecting to the outlet nozzles). The inner barrel is concentric with the reactor vessel and extends upward to an elevation approximately 1 m below the dip plate. Two sets of small holes penetrate the inner barrel in order to provide alternate flow paths that bypass the downcomer region. There are 48 symmetrically arranged set of lower holes with vertical position of their cylinder axis located approximately 1.6 m above the support plate, and an additional 24 holes with located approximately 2.5 m above the support plate.

The core barrel is a cylindrical structure that surrounds the reactor core. The upper core structure consists of a main housing that covers several structures including the control-rod drive mechanisms and guide tubes as well as the thermocouples and flow meters used to measure the fuel subassembly temperatures and flow rates.

### 2. Simplified Upper Plenum Geometry and the Test Specifications

In order to evaluate various computer programs and turbulence models using a common geometry by all participants, a simplified symmetric upper plenum model for the Monju reactor vessel was developed at Argonne. As shown in Figure 2, the simplified model includes only the region between the support plate at the bottom, and the dip plate on top (modelled as a solid wall instead of a free surface). The thickness of the reactor vessel is ignored and the inner barrel is modelled as an adiabatic gap in the flow domain (i.e., the conductive heat transfer through 40 mm thickness of the inner barrel is neglected).

To approximate symmetry, the fuel handling machine hold-down arm and lower guide, fuel transfer machine lower guide, in-vessel spent fuel storage racks, and the thermocouple plug are excluded in the simplified model. Also, the reactor outlet nozzle is rotated 12.5-degrees clockwise to align it symmetrically with respect to the hexagonal core configuration. One of the symmetry planes cuts the outlet nozzle in half. Although the outlet nozzle in the simplified model is considerably longer than what is shown in Figure 1, extending the outlet end of pipes/nozzles away from the computational domain is deemed to be important based on earlier experience to avoid the undue influence of the outlet boundary conditions on the upstream results.

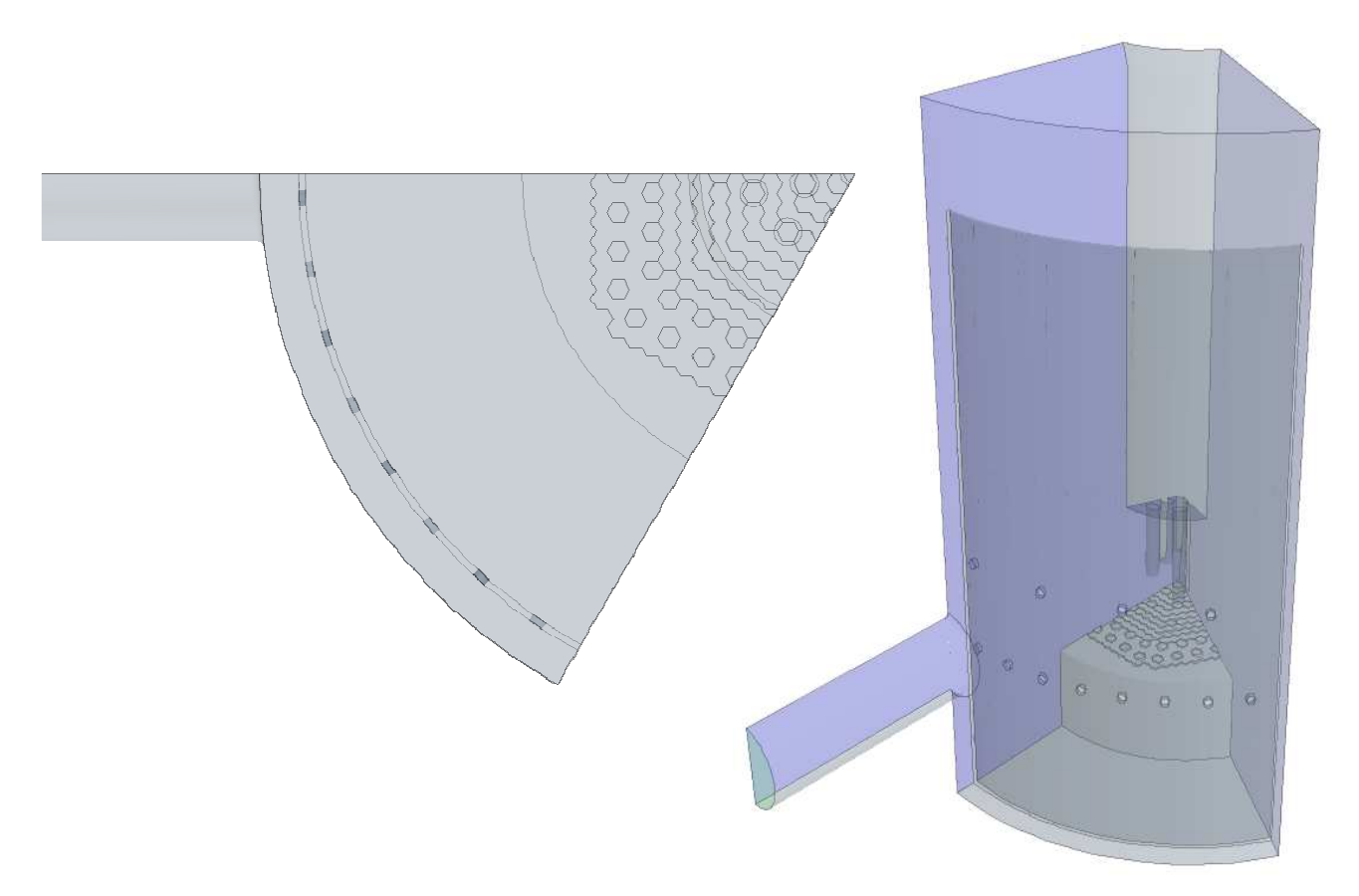


Figure 2 Top (left) and isometric view (right) of the Monju simplified upper plenum CAD model used as the common geometry for the benchmark CFD simulations.

The 1/6<sup>th</sup> symmetric segment (60° section) corresponds to the W-SW portion of the core. All of the subassembly outlets (inlets of the upper plenum model) are represented explicitly with their hexagonal shape to distinctly identify different inlet zones at the inner core, outer core, radial blanket subassemblies, neutron shielding zone, and control assembly outlets. Each of these inlet zones have a distinct flow rate and core outlet temperature specified as time dependent inlet boundary conditions for the upper plenum model.

The turbine trip test was initiated from 40% of nominal electric output condition to confirm a safety feature of the Monju plant against a turbine failure. The test also demonstrated the decay heat removal capability via sodium circulation in the primary and secondary heat transport loops using the sodium-air heat exchangers (installed in parallel with the steam generators) as the heat sink. During the test, significant thermal stratification in the reactor vessel was observed at the reduced primary system sodium flow rate (maintained through a pony motor) after the reactor was shutdown.

As part of the benchmark specifications, the distinct flow rates and core outlet temperatures for the inlet zones have been provided by JAEA as time-dependent inlet boundary conditions for the upper plenum model. Based on the assumed flow distribution and heat load among the core fuel subassemblies, blanket subassemblies, control rods, and neutron shields, the entire core is divided into total sixteen zones. The changes in per assembly sodium flow rate and temperatures in each inlet zone throughout the turbine trip test indicate a coast down (in about 20 seconds) of flow rates following the primary pump trip, and more gradual reduction in core outlet temperatures (in about a minute) following the reactor shutdown.

#### 3. CFD Mesh and Model

The volume mesh for the simplified model is built using various options. Starting with the CAD model shown in Figure 2, a finely triangulated surface mesh enclosing the volume occupied by the liquid sodium is prepared as the first step. This common surface mesh established the basis to generate volume meshes using both trimmed hexahedral and polyhedral cells, each with a coarse and a refined grid with total computational cell count ranging from 0.4 to 3.5 million. All volume meshes included local refinements around the upper core structure, in the outlet nozzle, and around the flow holes on the inner barrel. The steady-state calculations (to simulate the conditions before the test is initiated) are performed to assess sensitivity of the calculated results to the mesh structure.

Although the grid independent solutions are obtained with both types of meshes, the optimal CFD mesh of the Monju upper plenum is selected as the grid with polyhedral cells. The CFD mesh used for the subsequent transient simulations has 100 mm base (reference) cell size. Near the surfaces of various upper plenum components, additional constraints are specified to enforce local cell refinements. These constraints include minimum 36 points to represent the curvature of a circle and several volumetric controls to enforce reduced base cell size. Specifically, the base cell size is limited to 25 mm in the region just above the subassembly outlets and inside the outlet nozzle, 50 mm in the porous region representing the upper core structures, 12.5 mm in the transition region between the reactor vessel and outlet nozzle, and 6.25 mm around each flow hole to assure accurate representation of the pressure drop for bypass flow through them. "Medium" growth rate is specified to assure gradual transition between the bulk volume mesh and the regions with local refinements.

The polyhedral mesh has four layers of prismatic cells near the wall boundaries with 25 mm total thickness and 1.3 as the ratio of the thickness of consecutive layers (about 4 mm for the thickness of near-wall boundary layer). Around the holes through the inner barrel, 8 prismatic cell layers with a

total thickness of 20 mm is enforced using 1.25 as the ratio of the thickness of consecutive layers. Inside the outlet nozzle, 8 prismatic cell layers with a total thickness of 25 mm is enforced using 1.2 as the ratio of the thickness of consecutive layers. With these parameters, the final mesh has about 840,000 CFD cells as a reasonably refined near-optimal mesh suitable for simulations of hours long transient. Other than the larger control-rod guide tubes, the complex geometric structures above the core (flow guide tubes, honeycomb structure, thermocouples and flow meters, and fingers) are excluded. Instead, this crowded region is modelled using the porous media approach based on characterization of distributed resistance of various components as determined by CEA.[2]

The inlet boundary conditions at the core subassembly outlets are specified in user subroutines as the time dependent values for the sodium flow rates and subassembly outlet temperatures and linearly interpolated between the tabulated values. The subassembly mass flow rates (in kg/s) are converted to velocities (in m/s) by taking into account the proper density of the liquid sodium at the specified outlet temperature of the corresponding subassembly. These "superficial" velocities are then specified to apply uniformly at the subassembly outlet neglecting the effect of the reduced cross section flow area. This approximation is expected to underestimate the pressure drop near the subassembly outlets; however, it is consistent with the porous media representation of the upper core structures. Other than the two symmetry planes and the end of the outlet nozzle, all other boundaries in the simplified model are treated as adiabatic walls. The end of the outlet nozzle is modelled as flow-split outlet boundary to avoid any inflow due to temporal pressure fluctuations.

The calculations are performed using the realizable k-ɛ turbulence model with standard wall functions. The prismatic cell layers are used to provide appropriate wall boundary thicknesses suitable with the Reynolds-Averaged Navier-Stokes (RANS) turbulence models intended to be used in simulations. Also, the sharp edge between the outlet nozzle and reactor vessel is rounded to avoid large pressure fluctuations and recirculation around that edge. Most commercially available CFD software provide limited options for higher-order spatial discretization. In this study, the second-order proprietary MARS scheme is evaluated for both the initial steady-state and transient calculations. The algebraic set of finite volume equations resulting from discretization of conservation and turbulence transport equations are solved using the well-established Semi-Implicit Method for Pressure Linked Equations (SIMPLE) in conjunction with a first-order, fully-implicit Euler scheme. The SIMPLE method usually provides accurate results for lower computational cost, but a separate calculation using the more conventional Pressure Implicit with Splitting of Operators (PISO) transient solver scheme that involves predictor-corrector stages for each time step is also performed for comparisons. The algebraic multi-grid (AMG) solver is used to accelerate the convergence in both cases.

#### 4. Analysis Results for the Initial Steady-State

The steady-state calculations are completed to obtain the initial state from which the transient calculations are assumed to start, but also to assess the suitability of the CFD mesh for the simulation of expected natural convection conditions in the Monju upper plenum during the long transient. These initial simulations exhibited some convergence difficulties with both trimmed hexahedral and polyhedral mesh structures, requiring an approach to the initial (steady-state) solution by means of time steps. In the first stage, steady-state calculations are run to force the solver to achieve a time-averaged flow field and temperature distributions with limited convergence. In the second stage, a time-dependent null transient is computed for an additional one minute of simulation time to allow the solution to settle into one of its common modes of fluctuations typically observed in mixed convection flow regimes.

The velocity magnitude and temperature contour plots on the symmetry plane through the outlet nozzle, and on the horizontal plane that cuts through the lower holes on the inner barrel and the outlet nozzle, are shown in Figure 3. The results indicate a fairly large annular recirculation zone in the upper plenum where the hot plume from the core first spreads conically outward and then flows upward along the inner barrel's inner surface, followed by a downdraft along the vertical surface of the upper core structure main body. The flow field in the annulus between the inner barrel and reactor vessel is uniformly downward, converging toward the outlet nozzle. As expected, the small holes on the inner barrel do not play a significant role on mixing of the fluid on opposing sides of inner barrel for the initial steady-state conditions.

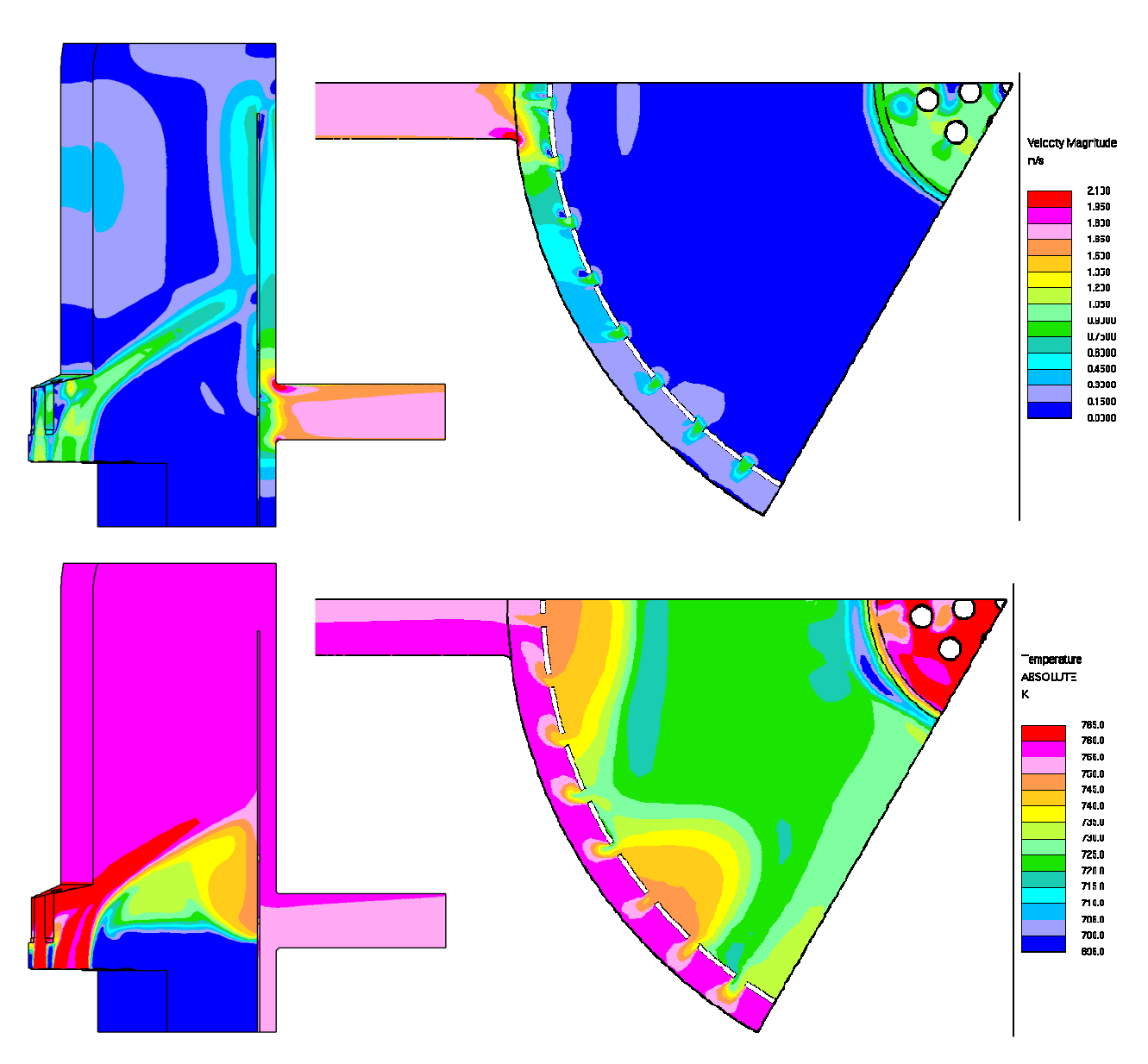


Figure 3 Velocity magnitude (top) and temperature contour plots (bottom) for the initial conditions on the symmetry plane through the outlet nozzle (left) and on the horizontal plane that cuts through the lower holes on the inner barrel (right).

The temperature plots indicate substantial thermal striping near the core subassembly outlets, but otherwise fairly uniform temperatures for the well-mixed flow in the bulk of the upper plenum. Although there is no major thermal stratification in the upper portion of the upper plenum initially, the results predict a significantly lower temperature for the stagnant sodium below the core barrel. The temperatures along the thermocouple tree (shown as TC plug in Figure 1) for the initial conditions are compared with the test data in Figure 4 for both the polyhedral and trimmed hexahedral meshes. The consistency of the results with both mesh types confirms the grid independence of the solutions.

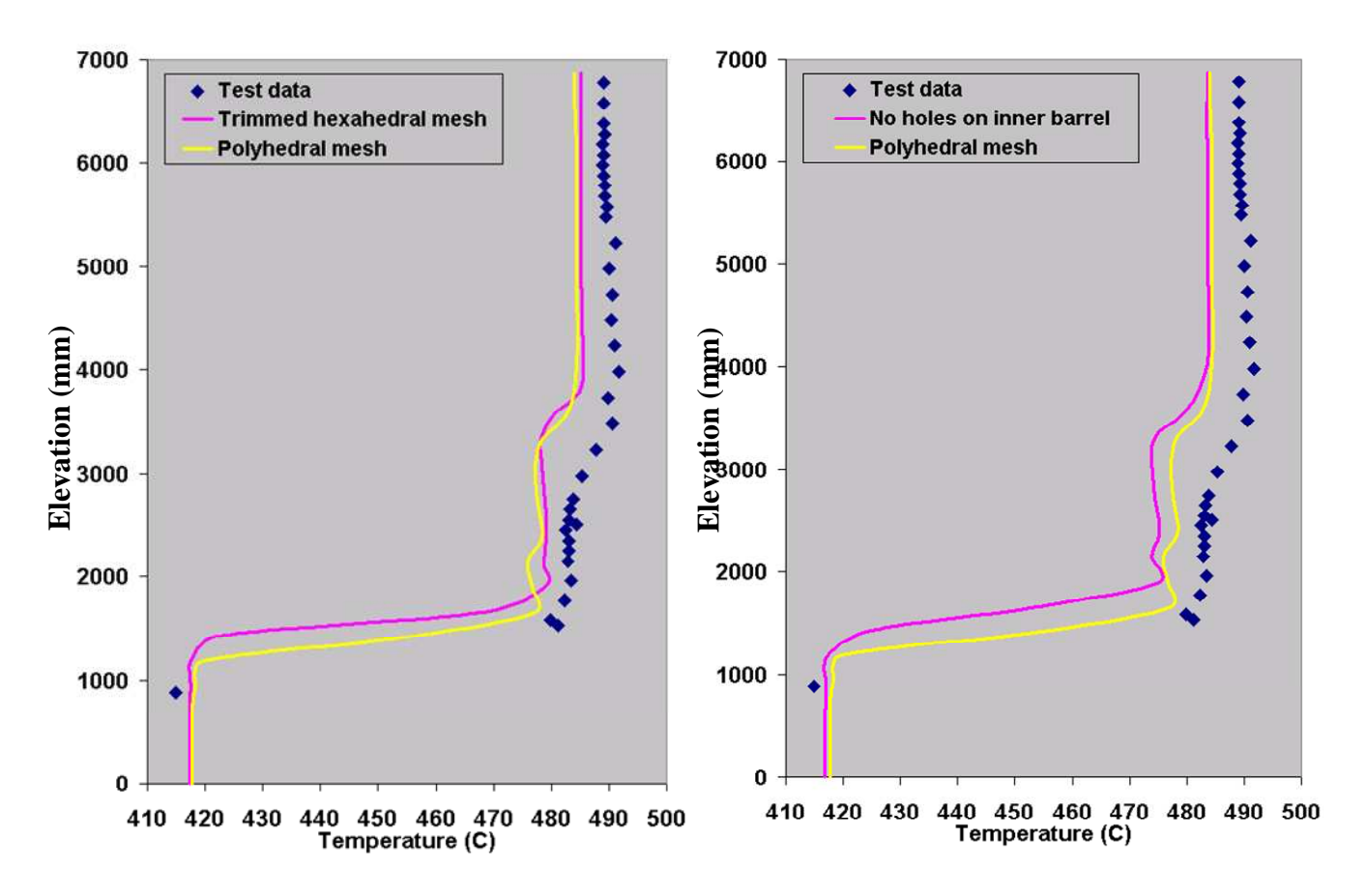


Figure 4 Comparison of temperature distributions along the thermocouple tree with various modelling options.

As seen in Figure 4, and in agreement with the code prediction, the test data indicates significantly more stratified liquid sodium in the reactor vessel below the core outlet with the only thermocouple at that elevation measuring about 75°C cooler temperature than what was measured in the upper part of the plenum. However, in the upper portion of the reactor vessel, the fairly uniform sodium temperature is predicted as 5°C cooler than the experimental data. Since most of sodium coolant in the upper plenum above the elevation of the holes on the inner barrel is at that temperature, this discrepancy corresponds to either an underestimation of flow through the bypass holes or about 4% energy imbalance for the initial steady-state conditions.

To address this discrepancy, importance of inner barrel holes to provide a bypass flow path for colder sodium (leaving the sodium hotter in higher elevations) was evaluated using a model with no holes. As shown in Figure 4, the model without inner barrel holes results in a similar temperature distribution, confirming the conclusion that the influence of holes is negligible at steady-state with full-flow. However, it does not rule out the possibility of greater bypass flow than what is predicted with the CFD model.

### 5. Results for Transient Analysis

The transient calculations started following a 60 seconds long null transient as explained in Section 4, and completed in several stages. The critical first minute of simulations (when the flow rate nominally drops down to 1/5th of the initial, steady-state value due to primary pump trip) is completed using 5 ms time steps. Following four minutes of the tests during which the core outlet temperature drops more than 100 K on average following the reactor shutdown and the flow rate coasts down to the natural circulation levels are simulated with 10 ms time steps. The remaining transient calculations are performed using 50 ms time steps.

The temperature contour plots on the symmetry plane through the outlet nozzle calculated with both SIMPLE and PISO transient solver options are shown in Figure 5 for various stages during the transient calculations. Despite a sudden drop in the flow rate through the core following the pump trip and subsequent flow coast-down, the temperatures in the upper plenum decrease at a much slower rate primarily due to thermal stratification. At the beginning of the transient, the bulk of the primary sodium in the upper plenum (except in lower elevations below the core outlet) is more or less at the same temperature, about 755 K. When the transient starts and core outlet temperature gradually drops due to reactor shutdown, the cooler (more dense) sodium stays near the bottom of the vessel and the hotter (and less dense) primary sodium at the higher elevations in the upper plenum stays largely stagnant. The calculations predict that the resulting thermally stratified mixing pattern prevails for about ten minutes into the transient.

Normally, the thermal stratification in the upper plenum impedes the natural circulation and degrades the passive safety performance of a reactor. When the colder and denser sodium is trapped at lower elevations, the upper plenum outlet temperature (as well as in the outlet nozzle) could stay high for a long period of time. Since the natural circulation flow rate in the primary system depends heavily on the temperature differential and elevation difference between the reactor core and main heat sink (in this case, the intermediate heat exchanger), a thermally stratified upper plenum translates to lower natural circulation flow rates.

In Monju design, however, two sets of holes on the inner barrel provide alternative flow paths between the core outlet and the IHX inlet nozzle, bypassing the thermally stratified region of the upper plenum which poses larger impedance to natural circulation flow patterns following a reactor shutdown. Because of these bypass flow paths through the holes on the inner barrel, the average temperature through the outlet nozzle (the inlet temperature into the intermediate heat exchanger) starts decreasing as early as two minutes into the transient while most of the upper plenum above the core remains hot. Once the colder sodium fills the annular gap between the reactor vessel and inner barrel below the elevation of the outlet nozzle, the average temperature in the outlet nozzle follows the average core outlet temperatures fairly closely.

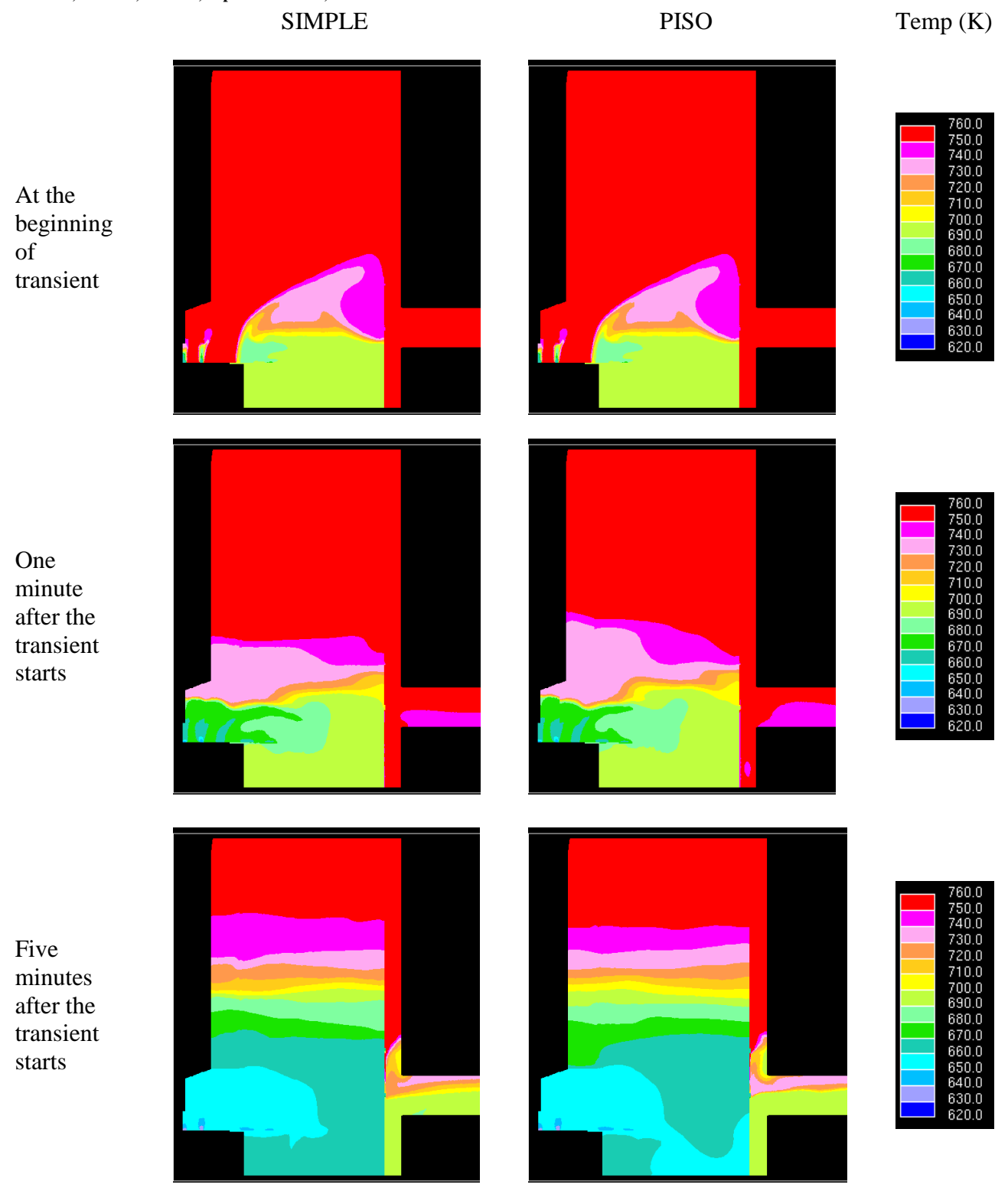


Figure 5 The temperature contour plots on the symmetry plane through the outlet nozzle for various stages during the transient calculations.

A comparison of the calculated transient temperatures along the thermocouple tree with the test data at various points during the test is shown in Figure 6. Although during the initial stages of the transient the calculated results are in reasonably good agreement with the test data along the entire height of the upper plenum, around the 5-minute mark, the discrepancy above the elevation of the holes on the inner barrel (2,550 mm) starts growing. Only 15 minutes into the transient, the calculations indicate fairly uniform sodium temperature almost along the entire height of the upper plenum except at elevations above the upper end of the inner barrel, whereas the test data shows still significant stratification at elevations above the holes on the inner barrel at that point. In fact, the test data indicates that the thermal stratification persists in the upper plenum for well over an hour.

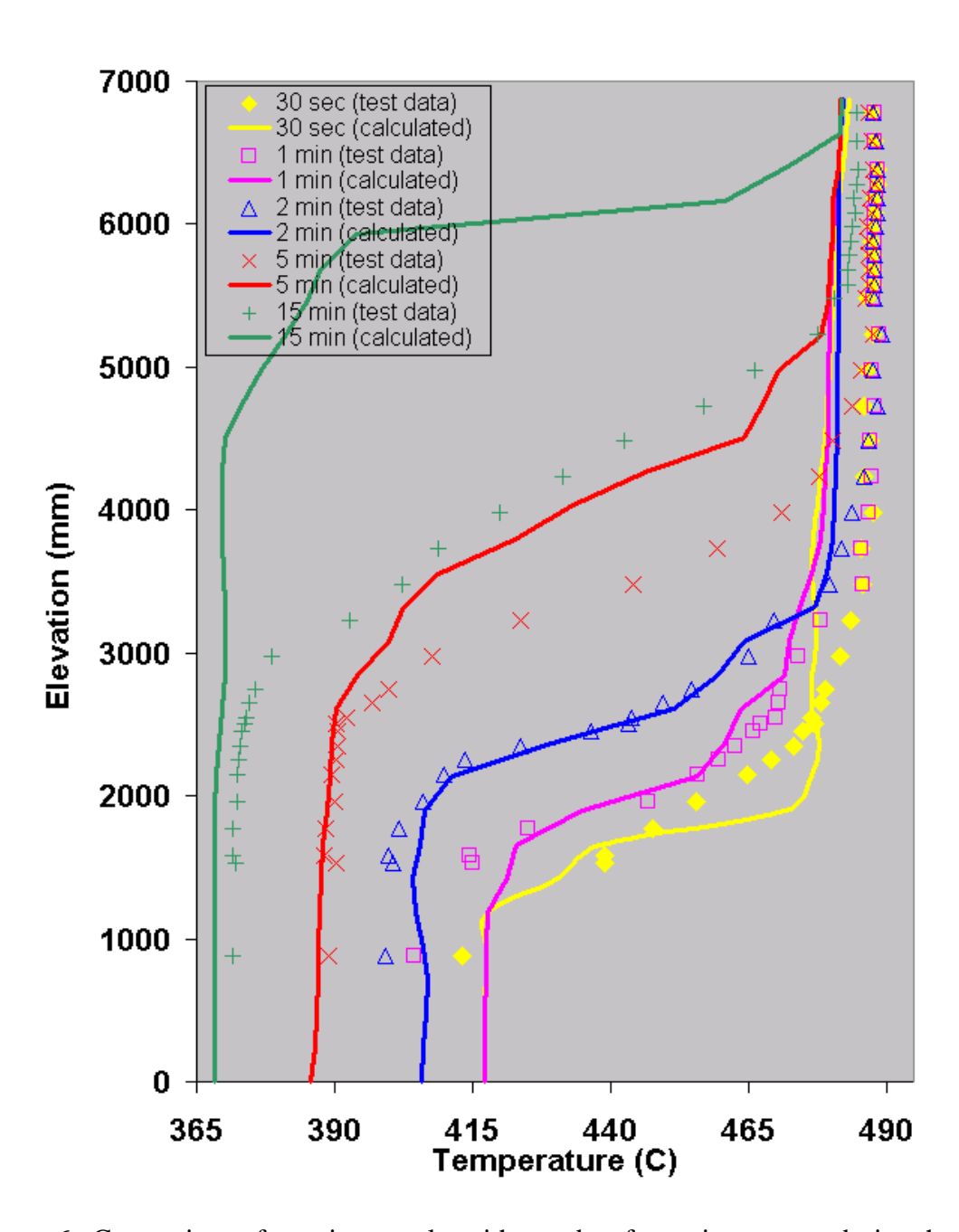


Figure 6 Comparison of transient results with test data for various stages during the test.

Consistency of the solutions with SIMPLE and PISO as seen in Figure 5 eliminates the transient solver option as the potential source of discrepancy. To assess the impact of turbulence modelling on the mixing, two additional set of simulations are also performed: one using a small constant value for the turbulent viscosity, and another with laminar flow. As expected, the case with small constant value for turbulent viscosity does not differ much from the earlier predictions since the impact of turbulent mixing dies down once the primary pump stops and turbulence dissipates. Although the laminar flow solution shows significant numerical instabilities, it is more or less consistent with the solutions with turbulence models and does not resolve the large discrepancy with the experiments for steady-state or transient phases of the simulations.

One plausible explanation of the discrepancies between the calculations and test data is that the bypass flow through the holes on the inner barrel is underestimated in the CFD model. If the bypass flow is greater than what is predicted in the simulations, it could account for a larger fraction of the primary system flow both before and after the turbine trip. The deflection point in the test data shown in Figure 6 at the elevation of upper holes somewhat supports this hypothesis (the sodium below the holes is fairly well mixed at uniform temperature while the sodium above the holes remain stratified for a much longer period). Since the holes in the CFD model are represented explicitly based on the benchmark specifications provided by JAEA, there is not much room for modifications. However, one idea is to assume rounded edge for the holes which could reduce the pressure drop by as much as 1/3 in comparison to the current configuration with sharp edged holes.

Another impact is expected due to the heat capacity and conjugate heat transfer of the major components in the Monju upper plenum. The stored heat in the upper core structure and the stagnant sodium above the dip plate, as well as the conjugate heat transfer through the inner barrel will likely make a difference in the predicted thermal stratification patterns. During the next phase of the benchmark project these effects will be included in the CFD simulations.

#### 6. Conclusions

The IAEA coordinated research project on the analysis of thermal stratification in Monju reactor provides an opportunity for validation of safety analysis models and methods using test data from a turbine trip test. A simplified Monju upper plenum model has been developed to serve as the baseline model for the initial evaluations of the candidate CFD software and methods. The simplified model includes a 60° symmetric segment of the Monju upper plenum excluding fuel handling and transfer system. The holes on the inner vessel barrel are represented explicitly as alternate flow paths to the down-comer region to capture the bypass flow. Other than the large cylindrical main body and the large-diameter control-rod guide tubes, the upper core structure components are represented via porous media models.

Following an optimization study focusing on grid size, temporal discretization (time step size), and parallel performance, a medium size model with 840,000 cells is used for the reference calculations using the standard high-Reynolds number k- $\epsilon$  turbulence model in conjunction with logarithmic wall-functions. The calculations for the initial (steady-state) conditions indicate a large annular recirculation zone with fairly uniform temperatures for the well-mixed flow in the upper plenum. When the transient starts and core outlet temperature gradually drops due to reactor shutdown, the cooler (more dense) sodium stays trapped near the bottom of the vessel while the hotter (and less dense) primary sodium at the higher elevations stays largely stagnant for an extended period of time. However, two sets of holes on the inner barrel provide alternative flow paths between the core outlet and outlet nozzle, bypassing the thermally stratified region of the upper plenum and improving the natural circulation flow rate.

Consistency of the solutions with different mesh types underscore that the grid-independent solutions have been obtained. However, there is about 5°C discrepancy between the test data and calculation results in the upper portion of the plenum (above the core outlet level) at steady-state and it indicates either about 4% energy mismatch or an underestimation of the bypass flow through the holes on the inner barrel.

The transient calculations were performed only with the polyhedral cell model but using both the SIMPLE and PISO solver options. Both set of calculations suggest a much shorter-term thermal stratification than the experimental data indicates. In the next phase of simulations, the major components in the upper plenum (upper core structure, core barrel, and inner barrel) will be modelled as solid structures with their own heat capacity and thermal conductivity. Perhaps more importantly, the importance of the holes on the inner barrel will be reassessed in terms of their ability to provide larger than currently predicted by-pass flow, leaving a longer term thermal stratification in the upper portion of the Monju upper plenum.

### 7. Acknowledgements

The submitted manuscript has been created by UChicago Argonne, LLC, Operator of Argonne National Laboratory ("Argonne"). Argonne, a U.S. Department of Energy Office of Science laboratory, is operated under Contract No. DE-AC02-06CH11357. The U.S. Government retains for itself, and others acting on its behalf, a paid-up nonexclusive, irrevocable worldwide license in said article to reproduce, prepare derivative works, distribute copies to the public, and perform publicly and display publicly, by or on behalf of the Government.

#### 8. References

- [1] STAR-CD Versions 4.08-12, http://www.cd-adapco.com/products/STAR-CD/, CD-adapco Inc, Melville, NY (2009-2011).
- U. Bieder, G. Fauchet, and S. Yoshikawa, "TRIO\_U ANALYSIS OF NATURAL CONVECTION IN THE UPPER PLENUM OF THE MONJU REACTOR", <u>Proceedings of the 14th International Topical Meeting on Nuclear Reactor Thermal Hydraulics (NURETH-14)</u>, Toronto, Ontario, Canada, 2011 September 25-29.